

RESEARCH NOTE

SEM and RHEED–REM Study of Au Particles Deposited on Rutile TiO₂(110) by Deposition Precipitation and Gas-Phase Grafting Methods

T. Akita,¹ M. Okumura, K. Tanaka, and M. Haruta

National Institute of Advanced Industrial Science and Technology, Midorigaoka 1-8-31, Ikeda, Osaka 563-8577, Japan

Received January 18, 2002; revised June 26, 2002; accepted July 9, 2002

In order to investigate the structural features of Au/TiO₂ catalysts, which are active for the low-temperature oxidation of CO and reverse water shift reaction, a model structure was prepared by deposition precipitation (DP) and gas-phase grafting (GG) methods using rutile TiO₂ single-crystal fragments with cleaved (110) faces. SEM (scanning electron microscope) and RHEED–REM (reflection high-energy electron diffraction–reflection electron microscope) observations proved that Au particles deposited by DP are nonhomogeneously dispersed while those by GG are homogeneously dispersed on the (110) surface of the rutile TiO₂. The RHEED pattern indicated that a preferred orientation between the Au particles and the TiO₂(110) was $[\bar{1}10](111)_{\text{Au}}//[001](110)_{\text{TiO}_2}$ for both preparation cases. © 2002 Elsevier Science (USA)

Key Words: Au; TiO₂; deposition precipitation; gas-phase grafting; SEM; RHEED–REM; orientation relationship.

1. INTRODUCTION

Since it was found that Au exhibited high catalytic activity when supported on metal oxides as nanoparticles with diameters of less than 10 nm (1), the heterogeneous catalysis of Au clusters and Au catalysts has attracted growing interest (2, 3). To prepare highly dispersed Au particles on the surfaces of metal oxide powders, deposition precipitation (DP) (4) and gas-phase grafting (GG) methods (5) are the among most convenient and efficient. Deposition precipitation is applicable only to neutral and basic metal oxides, such as TiO₂, Fe₂O₃, and MgO, while gas-phase grafting can be applied to almost all types of support materials, including activated carbon and acidic metal oxides such as Al₂O₃–SiO₂. These methods prefer powder metal oxide supports with high specific surface area. We carried out the structure analyses using various techniques in order to elucidate the correlation between the structure of the Au catalysts and their catalytic activity (6–11).

¹ To whom correspondence should be addressed. Fax: +81-727-51-9714. E-mail: t-akita@aist.go.jp.

Gold on TiO₂ is representative of gold catalysts because Au and TiO₂ alone does not exhibit high catalytic activity and the combination of the two components leads to unique catalytic properties for the CO oxidation (12), water gas shift reaction (13), and epoxidation of propylene (14).

In our previous study, the epitaxial orientation between Au particles and the TiO₂ support was studied by HRTEM (high-resolution transmission electron microscopy) for Au/anatase TiO₂ and Au/rutile TiO₂ powder catalysts (9). However, it is still difficult to clarify the general features of the Au particle structure and the contact structure between the Au particles and the TiO₂ substrate. Therefore, we have attempted to prepare better-defined model structures by depositing Au nanoparticles on a rutile TiO₂ single crystal using the DP and GG methods. Recently, a new method preparing size-controlled Au particles on a TiO₂ surface was developed by using Au–phosphine (15). These model structures made on TiO₂(110) allow detailed structural studies since the orientation of the TiO₂ support is known and its surface has atomically flat terraces and atomic steps. And they allow correlation of the results with those of STM (scanning tunneling microscopy) observations for well-defined TiO₂ surfaces (16, 17) and Au/TiO₂ system (18) studied under UHV condition.

It is also beneficial to correlate the structure and catalytic activity. Therefore the model structures in this study were prepared by the same method used for the preparation of powder catalysts for activity measurements.

In the present study, we observed the distribution of Au particles on the (110) surface of rutile TiO₂ by SEM and investigated the orientation relationship between the Au particles, TiO₂ support, and surface structure of Au/TiO₂(110) with RHEED (reflection high-energy electron diffraction)–REM (reflection electron microscope) (19). These techniques have advantages in obtaining an overview of the surface, although the resolution is not high enough for a structure analysis at the atomic level.

2. EXPERIMENTAL

Gold particles were deposited using the DP (4) and GG (5) methods. A single crystal of rutile TiO_2 commercially produced by Earth Chemical Co. was crushed in air and the cleaved (110) face was used as a substrate. In the DP method, a fragment of the TiO_2 single crystal was dipped in a 200-ml solution of aqueous HAuCl_4 (0.01 g/L), the pH of which was adjusted to 7 by adding NaOH solution. The dispersion was aged at 343 K for 1 h. In the GG method, an acetylacetonate complex of Au, $(\text{CH}_3)_2\text{Au}(\text{CH}_3\text{COCH}_2\text{COCH}_3)$, abbreviated $\text{Me}_2\text{Au}(\text{acac})$, was placed in the gas phase at 301–302 K in a vessel containing fragments of the rutile single crystal. Both the $\text{Au}(\text{OH})_3$ and $\text{Me}_2\text{Au}(\text{acac})$ samples deposited on $\text{TiO}_2(110)$ were calcined in air at 573 K for 4 h.

Although the composition analyses of the Au/TiO_2 surface has not been done, the amount of residual Na or Cl is always under the detection limit of XPS measurement for the powder catalyst prepared by the DP method. For the Au/TiO_2 sample prepared by the GG method, the residual

hydrocarbons are removed by decomposition during calcination in air (5).

These Au/TiO_2 samples were observed by SEM (Hitachi S-5000) at 20 kV and RHEED-REM (Hitachi H-9000NAR) at an accelerating voltage of 200 kV. TEM observations were also done in order to estimate the particle size and the amount of Au.

3. RESULTS AND DISCUSSION

Figure 1 shows SEM images of Au/TiO_2 prepared by the DP and GG methods. Gold particles are seen as bright contrasts. The spatial resolution of SEM was about 2 nm; thus the Au particles under 2 nm were not observed by SEM. TEM observation was also done for the Au particles on a TiO_2 single crystal prepared by DP and GG. It revealed that Au particles under 2 nm were seldom observed in this preparation condition. The different features in the dispersion of Au particles are clearly seen between the DP and GG methods. Gold particles deposited by DP shows inhomogeneous dispersion while those by GG are homogeneously

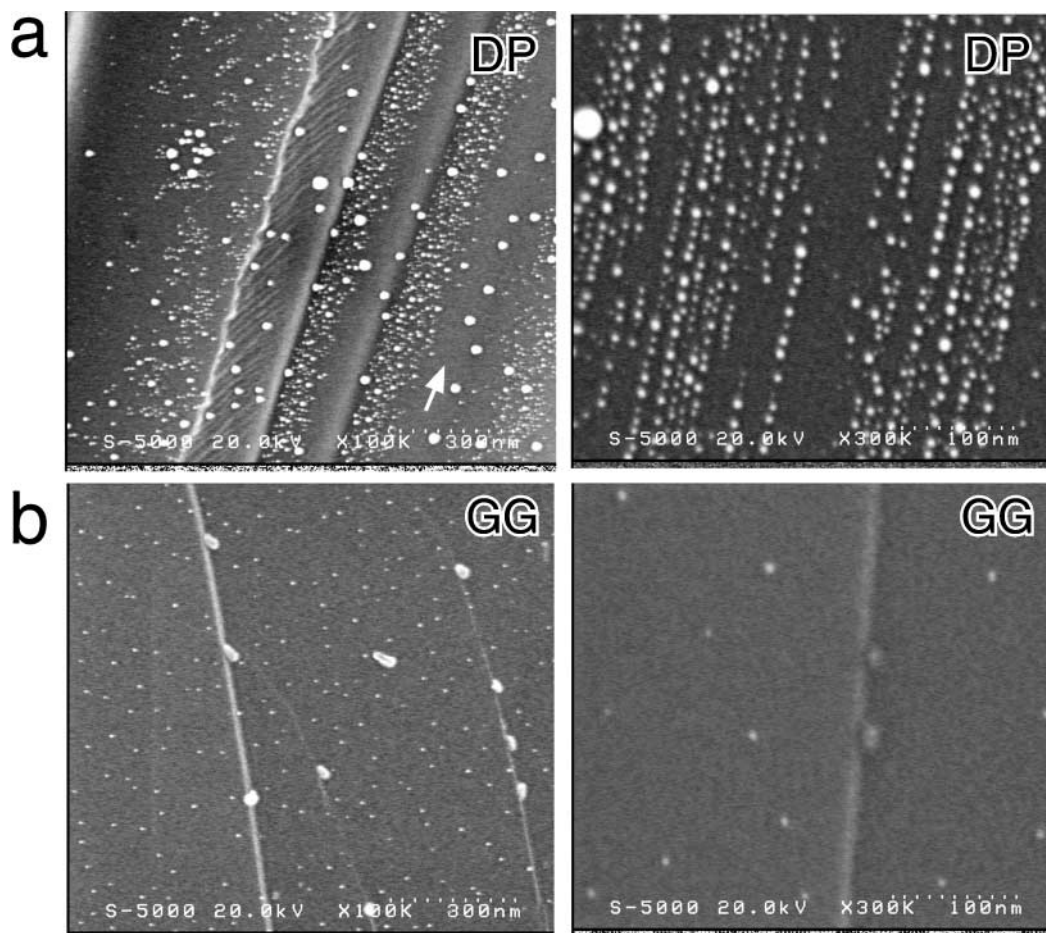


FIG. 1. SEM images of the $\text{Au}/\text{TiO}_2(110)$ surface prepared by DP (a) and GG (b) methods.

dispersed. This means that the Au particles deposited by DP are strongly affected by the surface structure and states of the TiO₂ substrate. It is hard to observe the monoatomic steps by SEM and the lines shown in the SEM images are multiple atomic steps. Sometimes Au particles are ordered along the straight line, as shown in Fig. 1a. It has not been proved what is effective for the ordering of Au particles, since the morphology of the TiO₂ surface, such as atomic steps, was not observed in this image. The size of the Au particles was also inhomogeneous depending on the population and it is much larger in the area indicated by the arrow in Fig. 1a than in the other areas. This indicates that the Au clusters readily moved on the TiO₂ surface during the calcination process in the former area.

The nonuniform distribution is caused not only by the difference in the mobility of the Au atoms, but also by the deposition amount of Au. It was estimated by measuring the size distribution from the SEM images and by calculating the total amount of Au that the amount of Au initially deposited on the TiO₂ surface from an aqueous solution of HAuCl₄ is different depending on the location. It is speculated from the inhomogeneous distribution of Au particles that the DP method is sensitive to the surface states, since the principle of the DP method is based on ions and the surface charge (4), while Au precursors are directly deposited from gas phase without apparent coulomb interac-

tion in the GG method. The precursor of Au, existing as mainly Au(OH)₄⁻ in the solution for the DP method, can be preferentially deposited on the sites of the TiO₂ surface which are positively charged. For the DP and GG methods, the catalyst precursors before calcination exist as Au(OH)₃ and Me₂Au(acac), respectively, and the growth process during calcination in air must be different from the process studied in the UHV system (20, 21). The decomposition of Au(OH)₃ and Me₂Au(acac) into metallic Au particles takes place during calcination in the DP and GG methods, and because calcination was carried out in air, the growth kinetics of the Au particles may be more complicated. Details about the calcination process of Au on the TiO₂ system prepared by DP and GG will be proved by *in situ* experiments.

Figure 2 shows REM images of the Au/TiO₂(110) surface prepared by the DP and GG methods. The incident electron beam is nearly parallel to the TiO₂[001] direction, which is perpendicular to the REM image. The REM image is formed by using an enhanced (880) Bragg reflection. The intensity of the reflected electrons is strong enough for the surface, which was set in the specimen chamber of the electron microscope immediately after calcination. For the Au/TiO₂ prepared by GG, decomposition of the precursor and combustion of the residual hydrocarbon occurs at around 400 and 550 K(5). Figure 2c shows Au particles with diameters of 5–20 nm as dark contrasts with mirror

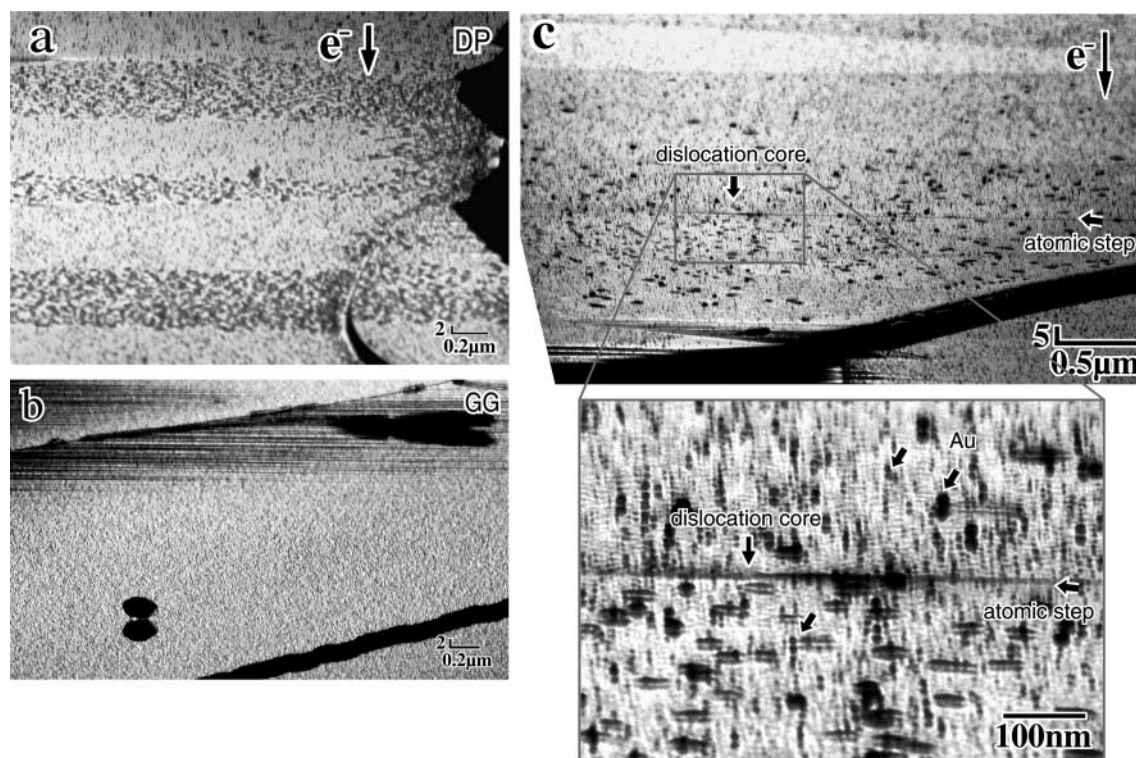


FIG. 2. REM images of the Au/TiO₂(110) surface prepared by DP (a) and GG (b) methods and the Au/TiO₂(110) surface with screw dislocation and atomic step prepared by the DP (c) method.

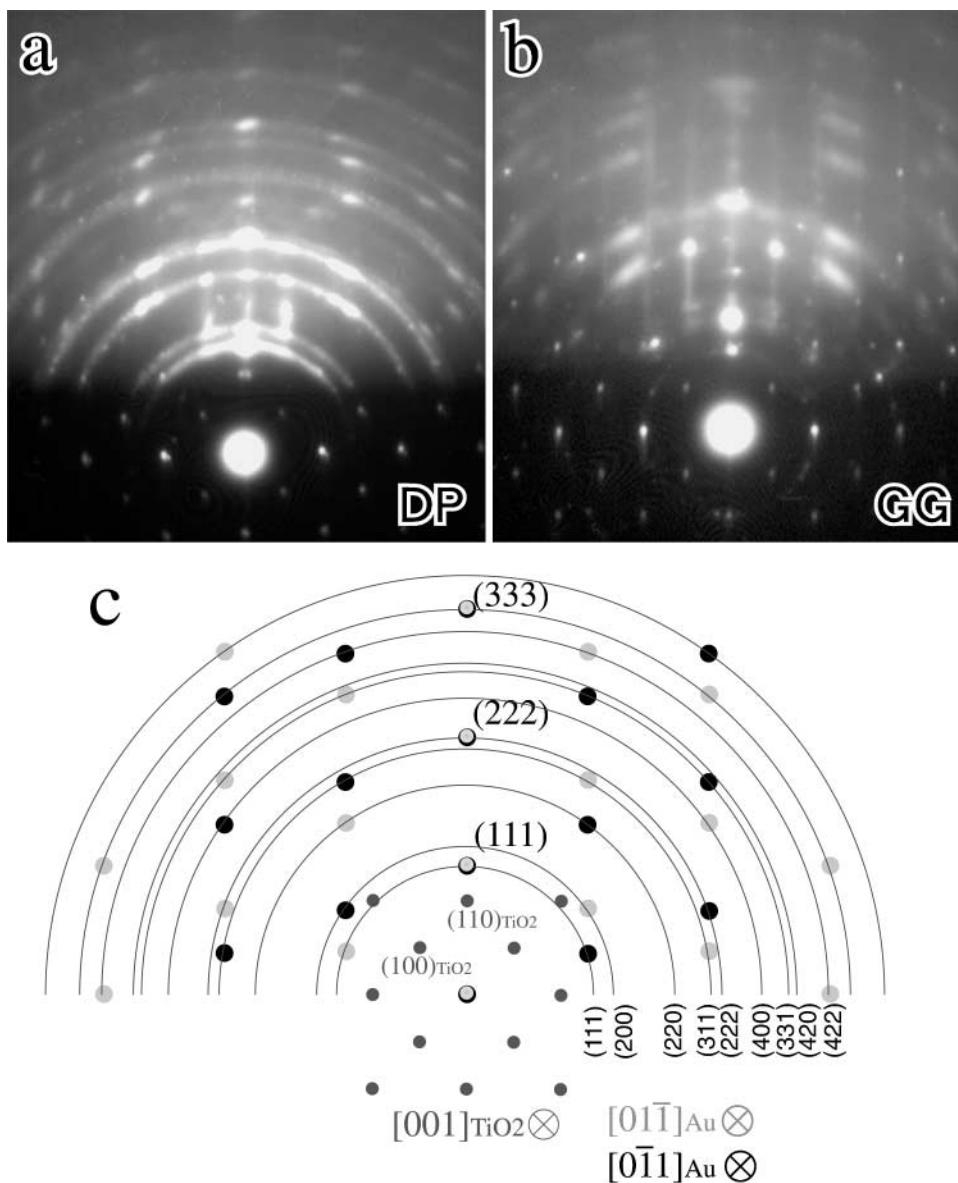


FIG. 3. RHEED patterns obtained from the Au/TiO₂(110) surface prepared by DP (a) and GG (b) methods and a schematic drawing of the RHEED pattern (c).

images in the Au/TiO₂(110) surface prepared by DP. The screw dislocation with monoatomic step was observed (22). The surface was gradually covered by contaminants during observation and the image became unclear. When the sample was again calcined at 573 K in air, the intensity of the reflected electron from the surface and image contrast was improved. This means that calcination in air is effective for cleaning the TiO₂ surface by removing the contaminants. It also seems that the arrangement of the surface atoms is relatively ordered based on the image contrast of the REM and RHEED pattern. Of course, details about the surface structure should be discussed along with the experiment under UHV conditions. No effect of the monoatomic step

and screw dislocation on the population of Au particles was seen. Since the feasible morphological inhomogeneity of the TiO₂ surface except for steps and dislocation is point defects such as an oxygen defect (23) or impurities, it seems that the population of Au particles depends on the number of point defects causing the change of charge distribution locally, which were not detected by SEM and RHEED-REM, for the Au/TiO₂(110) prepared by the DP method.

Figures 3a and 3b show RHEED patterns obtained from the Au/TiO₂(110) surfaces prepared by DP and GG. The incident electron was nearly parallel to the TiO₂{001} zone axis. The extra spot by surface reconstruction, such as the (2 × 1) structure observed under UHV conditions (16, 17),

was not seen in these RHEED patterns. Transmission diffraction rings from the fcc crystalline Au particles were observed and comparably strong diffraction spots were also observed on the diffraction ring. The intensity of the diffraction pattern is different between the Au deposited by DP and that deposited by GG. This is because the amount and sizes of the Au particles in DP are larger than those of the Au particles made by GG. The amount of Au was estimated by TEM observations and the amount of Au deposited by DP is 1.5–3.0 times greater than that by GG. The mean diameter of the Au particles was 11 and 4.2 nm for DP and GG, respectively.

Figure 3c shows a schematic drawing of a RHEED pattern along with the diffraction index. Diffraction spots are formed from the Au particles and the incident electron is parallel to the Au[01 $\bar{1}$] and Au[0 $\bar{1}$ 1] directions. The Au(111) spots are perpendicular to the TiO₂(110) surface; thus the Au particles have a tendency to be deposited with the orientation relationship (111)_{Au}//(110)_{TiO₂}. Cosandey *et al.* reported that Au particles deposited on a clean TiO₂(110) surface under UHV conditions were grown on TiO₂(110) with epitaxial orientations of (111)_{Au}//(110)_{TiO₂} or (112)_{Au}//(110)_{TiO₂} depending on the annealing temperature and its process (24). In our samples prepared by DP and GG, the preferred orientation relationship between the Au particles and TiO₂(110) was the same as their result.

The lattice constants of 0.144 nm for Au(220) and 0.148 nm for TiO₂(002) are very close and the lattice misfit is 2.7% in the direction of TiO₂ [001]. In the direction of TiO₂[1 $\bar{1}$ 0], the Au(211), 0.167 nm, is also close to the TiO₂(220), 0.162 nm, and the misfit is 3%. Thus it seems that this orientation relationship forms one of the stable contact structures. These model structures are useful for investigating the surface structure of Au/TiO₂(110), especially for investigating various phenomena, such as structural changes caused by a catalytic reaction and by deactivation of the catalyst, by direct comparison with the Au/TiO₂ catalyst using a powder support.

4. SUMMARY

The model structure of Au/TiO₂(110) was prepared by deposition precipitation and gas-phase grafting, which was used for the Au catalyst supported on a powder metal oxide support. SEM and RHEED-REM observations determined the following structural features.

1. Gold particles deposited by DP showed nonhomogeneous dispersion depending on the surface structure and states, while Au particles deposited by GG showed a homogeneous dispersion.

2. The preferred orientation relationship between the Au particles and the TiO₂(110) was [$\bar{1}$ 10](111)_{Au}//[001](110)_{TiO₂}.

REFERENCES

1. Haruta, M., Kobayashi, T., Sano, H., and Yamada, N., *Chem. Lett.* **405** (1987).
2. Bond, G. C., and Thompson, D. T., *Catal. Rev.-Sci. Eng.* **41**, 319 (1999).
3. Haruta, M., *Catal. Today* **36**, 153 (1997).
4. Tsubota, S., Haruta, M., Kobayashi, T., Ueda, A., and Nakahara, Y., in "Preparation of Catalysts V" (G. Poncelet, P. A. Jacobs, P. Grange, and B. Delmon, Eds.), p. 695. Elsevier, Amsterdam, 1991.
5. Okumura, M., Nakamura, S., Tsubota, S., Nakamura, T., and Haruta, M., in "Preparation of Catalysts VII" (B. Delmon *et al.*, Eds.), p. 277. Elsevier, Amsterdam, 1998.
6. Kageyama, H., Tsubota, S., Kamijo, N., and Haruta, M., *Jpn. J. Appl. Phys.* **32**, Suppl. 32-2, 445 (1993).
7. Vogel, W., Cunningham, D. A. H., Tanaka, K., and Haruta, M., *Catal. Lett.* **40**, 175 (1996).
8. Kobayashi, Y., Nasu, S., Tsubota, S., and Haruta, M., *Hyperfine Interact.* **126**, 95 (2000).
9. Akita, T., Tanaka, K., Tsubota, S., and Haruta, M., *J. Electron. Microsc.* **49**, 657 (2000).
10. Akita, T., Lu, P., Ichikawa, S., Tanaka, K., and Haruta, M., *Surf. Interface Anal.* **31**, 73 (2001).
11. Boccuzzi, F., Chiorino, A., Manzoli, M., Lu, P., Akita, T., Ichikawa, S., and Haruta, M., *J. Catal.* **202**, 256 (2001).
12. Haruta, M., Tsubota, S., Kobayashi, T., Kageyama, H., Genet, M., and Delmon, B., *J. Catal.* **144**, 175 (1993).
13. Sakurai, H., Ueda, A., Kobayashi, T., and Haruta, M., *Chem. Commun.* 271 (1997).
14. Hayashi, T., Tanaka, K., and Haruta, M., *J. Catal.* **178**, 566 (1998).
15. Fukui, K., Sugiyama, S., and Iwasawa, Y., *Phys. Chem. Chem. Phys.* **3**, 3871 (2001).
16. Onishi, H., and Iwasawa, Y., *Surf. Sci.* **313**, L783 (1994).
17. Onishi, H., Fukui, K., and Iwasawa, Y., *Bull. Chem. Soc. Jpn.* **68**, 2447 (1995).
18. Valden, M., Lai, X., and Goodman, D. W., *Science* **281**, 1647 (1998).
19. Wang, Z. L., "Reflection Electron Microscopy and Spectroscopy for Surface Analysis." Cambridge Univ. Press, Cambridge, U.K., 1996.
20. Parker, S. C., Grant, A. W., Bondzie, V. A., and Campbell, C. T., *Surf. Sci.* **441**, 10 (1999).
21. Zhang, L., Persaud, R., and Madey, T. E., *Phys. Rev. B* **56**, 10549 (1997).
22. Osakabe, N., Tanishiro, Y., Yagi, K., and Honjo, G., *Surf. Sci.* **102**, 424 (1981).
23. Fukui, K., Onishi, H., and Iwasawa, Y., *Phys. Rev. Lett.* **79**, 4202 (1997).
24. Cosandey, F., Zhang, L., and Madey, T. E., *Surf. Sci.* **474**, 1 (2001).